Progress In Electromagnetics Research C, Vol. 28, 47–60, 2012

COMPACT MULTI-BAND LOOP ANTENNAS USING CPW-BASED CRLH QUARTER-WAVE TYPE RESONATORS

S.-X. Liu and Q.-Y. Feng*

School of Information Science and Technology, Southwest Jiaotong University, Chengdu, Sichuan 610031, China

Abstract—In this paper, a novel approach to design compact multi-band loop antennas is proposed. This type of antennas is composed of coplanar waveguide (CPW)-based composite right/left-handed (CRLH) quarter-wave type resonators, and developed on a vialess single layer. Both size reduction and low frequency ratios have been achieved, profiting from the employment of quarter-wave resonators and the high nonlinearity in the left-handed region of CRLH transmission line (TL) dispersion diagram. A sample prototype operating at three negative modes (1.92/2.15/2.64 GHz) with an overall size of $29 \times 21.3 \times 1.0\,\text{mm}^3$ was manufactured and measured. Measured results show good agreement with EM simulation, exhibiting good impedance matching as well as stably omni-directional radiation patterns at the three operating modes.

1. INTRODUCTION

In the near future, a variety of wireless applications will be integrated into one handheld terminal, which leads to a great demand in designing antennas with multi-band, low profile, high performances, and easy to integrate in the devices [1]. Multi-band antennas with frequency notched function are useful for wireless applications since a single antenna can cover several different frequency bands while noise interference at frequencies outside of the selected band can be suppressed [2].

During the last years, multi-band antennas with good radiation characteristics have been developed widely and rapidly for wireless

Received 22 January 2012, Accepted 12 March 2012, Scheduled 19 March 2012

* Corresponding author: Quanyuan Feng (fengquanyuan@163.com).

applications [3–17]. Generally, the multi-band operations are achieved by adopting multi-branched strips [3–5] and adding parasitic elements [6–9] to resonate at different frequencies in a single radiating device. Slots with various shapes have been cut in the radiated patch or ground plane to obtain multiple resonances [10–14]. However, these solutions generally suffer from certain drawbacks, including a large volume, a large ground plane, and a large frequency ratio. Recently, the frequency-tunable/reconfigurable antennas have been proposed for multi-band wireless applications due to their characteristics of frequency selectivity and out-of-band noise rejection [15, 16]. However, this approach is trade-off with an increased fabrication complexity and an increased cost associated with switches and bias circuits. Additionally, very small elements that excite the ground plane are used for multi-band performance [17].

One possible solution to realize compact multi-band antennas with low frequency ratios could be utilization of metamaterial cells. Metamaterials possess unique properties compared with conventional nature materials, such as anti-parallel phase and group velocities, a zero propagation constant, and a nonlinear dispersion relation, which can be implemented by utilizing split ring resonators (SRRs) or CRLH TLs [18–20]. Several multi-band antennas loaded with SRRs have been proposed in [21–23]. In more details, in [21], a great reduction of operating frequency has been obtained by loading SRRs, but still suffers from big frequency ratios. Although frequency ratios lower than 1.07 have been achieved in [22], it is difficult to apply them in modern wireless applications because of high operating frequencies. CRLH TLs are able to easily achieve those aforementioned properties by employing circuit parameters. Most CRLH antennas reported to date have been leaky-wave antennas (LWAs) [24, 25] and zeroth-order resonator antennas (ZORAs) [26, 27], however, a little work has been recently done on CRLH multi-band antennas. In [28], a multi-band antenna using defected ground structure (DGS) D-CRLH TL is designed, exhibiting low frequency ratios and good performances. Unlike other proposed approaches, the CRLH TL approach offers a more straight forward design approach based on the dispersion diagram of the unit cell.

In this paper, a conceptual route for multi-band operation is presented. The basic building block is a CPW-based CRLH quarter-wave type resonator, which is implemented by CRLH TL with one side open circuited and the other side short circuited in a CPW configuration. The proposed resonator can provide good performances, such as multi-modes, small size, low frequency ratios, and easy fabrication. By modifying the unit cell and/or the number of unit cells,

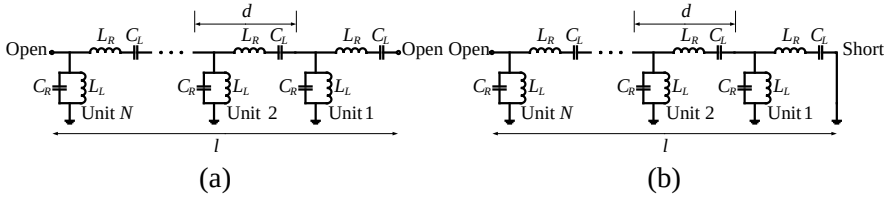

Figure 1. Circuit model of the CRLH TLs. (a) Conventional CRLH TL with both sides open circuited. (b) Proposed CRLH TL with one side open circuited and the other side short circuited.

more working frequencies with low frequency ratios can be arbitrarily chosen while only a little size is increased. To validate this approach, the tri-band sample was fabricated and measured. The simulated and measured results are presented and discussed as well.

2. CPW-BASED CRLH QUARTER-WAVE TYPE RESONATORS

The CRLH quarter-wave type resonator is firstly introduced in [29] to realize a miniaturized diplexer and a miniaturized triplexer. Figure 1(a) shows the conventional CRLH TL consisting of the series capacitance (C_L) and inductance (L_R) as well as the shunt capacitance (C_R) and inductance (L_L) with open boundary condition at both ends, where the subscripts L and R stand for left and right, respectively. As shown in Figure 1(b), the proposed CRLH TL is composed of a series resonant circuit and a shunt resonant circuit as well, but connected on the open side and shorted to the ground on the other side.

Like any TLs, a CRLH structure is transformed into a resonator when it is open-ended or short-ended. In a conventional CRLH TL with both sides open circuited (half-wave type resonator) [20], the resonance frequencies ω_n correspond to the frequencies where the physical length l of the structure is a multiple of half a wavelength or, equivalently, the electrical length $\theta = \beta_n l$ is a multiple of π

$$l = |n|\frac{\lambda}{2} \text{ or } \theta = \beta_n l = \beta_n N d = \left(\frac{2\pi}{\lambda}\right) \cdot \left(\frac{n\lambda}{2}\right) = n\pi \qquad (1)$$

with

$$n = 0, \pm 1, \pm 2, \ldots, \pm(N-1)$$

where n, N, d, and β_n are the resonance order, number of unit cells, physical length of each unit cell, and phase constant of CRLH TL, respectively. In principle, all of the $2N-1$ resonance modes may be

excited if matching condition is satisfied. The modes of each $\pm|n|$ pair have the same guided wavelength and field distribution, which would be very helpful for designing a multi-band antenna with good impedance matching and similar radiation characteristics [24].

However, for the proposed CRLH TL with one side open circuited and the other side short circuited (quarter-wave type resonator), the resonance condition is different from the conventional one, which is given as follows:

$$l = |n|\frac{\lambda}{4} \text{ or } \theta = \beta_n l = \beta_n N d = \left(\frac{2\pi}{\lambda}\right) \cdot \left(\frac{n\lambda}{4}\right) = n\pi/2 \qquad (2)$$

with

$$n = \pm 1, \pm 3, \pm 5, \ldots, \pm(2N-1)$$

where n, N, d, and β_n are the same with previously described. Note that this one exhibits similar $2N$ resonance modes, but the resonance order n can only be an odd integer. As compared to the conventional CRLH half-wave type resonator, this one is only half the size of the half-wavelength counterpart resonating at the same frequency. Therefore, the proposed CRLH quarter-wave type resonator is suitable to implement compact multi-band antennas.

To realize the physical structure of the proposed resonator in Figure 1(b), a CPW configuration where vias are not required is illustrated in Figure 2. It is composed of three main segments, including top metallic patches, shorted meander lines, and a CPW ground plane. The meander lines are connected between the top patches and the CPW ground plane to realize the shunt inductance (L_L). The gaps between the patches of the unit cell are designed for the series capacitance (C_L). The metallic patches contribute the series

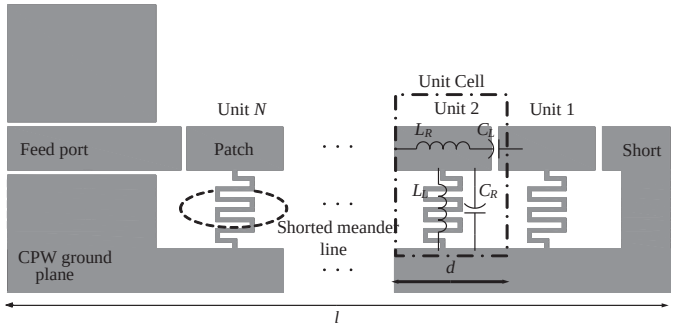

Figure 2. Structure of the proposed CPW-based CRLH quarter-wave type resonator.

inductance (L_R) while the shunt capacitance (C_R) can be found in the coupling between the patches and the CPW ground plane as well as the spacing of the meander lines. Note that this structure is inspired from [26] where the CRLH TL is applied to achieve a ZOR antenna.

To further investigate the characteristics of the proposed resonator, a lumped parameter extraction process of the CRLH TL unit cell is executed. Firstly, the values of inductances (L_L, L_R) and capacitances (C_L, C_R) can be approximately calculated according to [30], then each value is optimized based on the EM simulation results using a simple genetic algorithm (SGA) [31]. Figure 3(a) shows the physical dimensions of the CPW-based CRLH TL unit cell ($d = 3.4\,\text{mm}$). The extracted parameters using the above method account for $L_L = 2.77\,\text{nH}$, $L_R = 1.24\,\text{nH}$, $C_L = 0.36\,\text{pF}$, and $C_R = 1.13\,\text{pF}$. Based on these extracted parameters and dispersion relation of the CRLH TL [20], the left-handed region of dispersion diagram for the proposed unit cell is depicted in Figure 3(b). It can be observed that the phase shift per unit cell is nonlinear with frequency ($1.85 \sim 2.85\,\text{GHz}$), which leads to nonlinear ratios between resonant harmonics. According to (2), there will be N negative resonance modes when N unit cells are incorporated into the resonator. For example, with $N = 3$ unit cells, the proposed resonator will generate

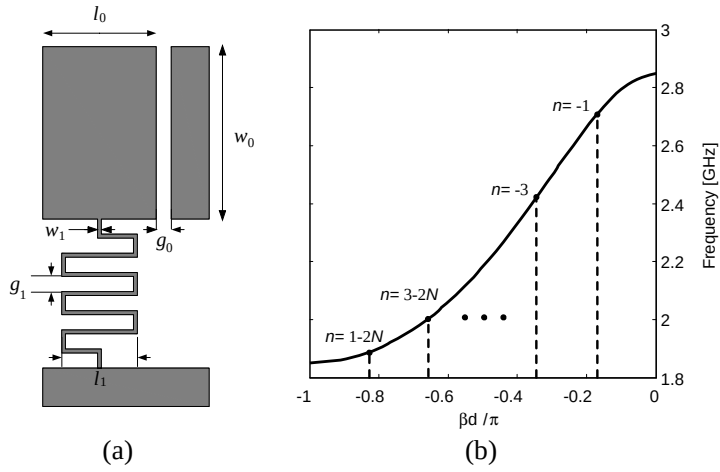

Figure 3. (a) Physical dimensions of the CPW-based CRLH TL unit cell: $l_0 = 3\,\text{mm}$, $w_0 = 4.5\,\text{mm}$, $g_0 = 0.4\,\text{mm}$, $l_1 = 2\,\text{mm}$, $w_1 = 0.1\,\text{mm}$, and $g_1 = 0.4\,\text{mm}$. (b) Left-handed region of dispersion diagram for the proposed unit cell and potential resonance modes for the proposed resonator.

$n = -1, -3, -5$ modes. Since these resonance frequencies are related to the dispersion diagram of the corresponding CRLH TL unit cell, the proposed resonator is capable of engineering the frequencies very close to each other by carefully modifying the unit cell, which makes it suitable to implement compact multi-band antennas with low frequency ratios. In addition, the CPW configuration provides high design freedom of reactance parameters that the inductance (L_L) and capacitance (C_L) can be easily adjusted by manipulating the length of the meander lines and the gaps between the patches, respectively, which results in an arbitrary slope of the left-handed curve in the dispersion diagram.

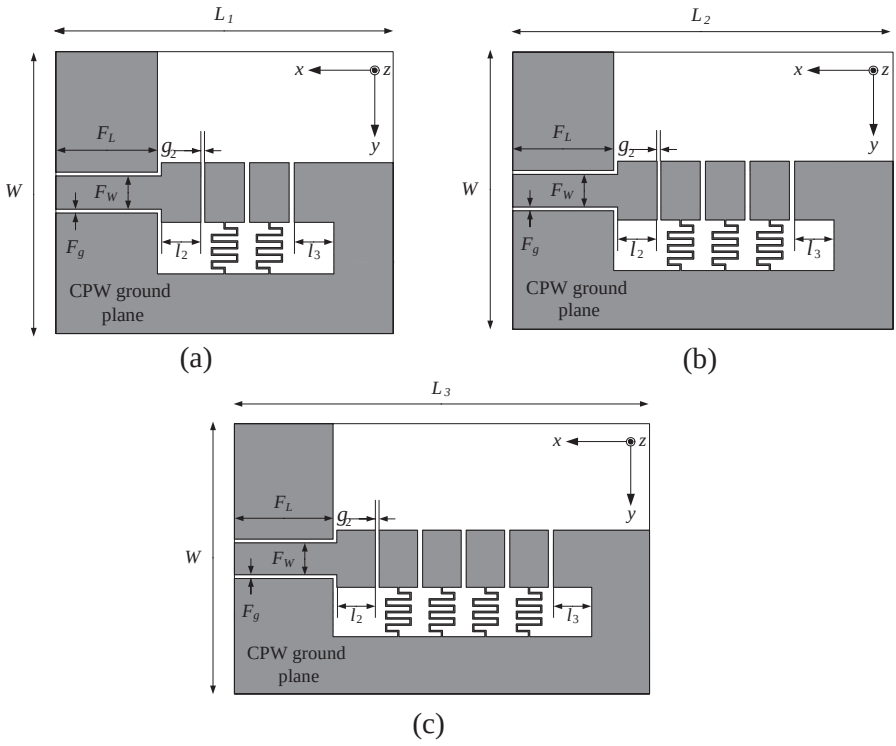

Figure 4. (a) Dual-band loop antenna. (b) Tri-band loop antenna. (c) Quad-band loop antenna. Their dimensions are as follows: $L_1 = 25.6\,\text{mm}$, $L_2 = 29\,\text{mm}$, $L_3 = 32.4\,\text{mm}$, $W = 21.3\,\text{mm}$, $F_L = 7.7\,\text{mm}$, $F_W = 2.5\,\text{mm}$, $F_g = 0.3\,\text{mm}$, $g_2 = 0.3\,\text{mm}$, $l_2 = 3\,\text{mm}$, and $l_3 = 3\,\text{mm}$.

3. DESIGN OF COMPACT MULTI-BAND LOOP ANTENNAS

Based on the proposed resonator, three prototypes of compact multi-band loop antennas are designed on FR-4 Epoxy substrates with a dielectric constant of 4.4 and a thickness of 1 mm, as illustrated in Figure 4. They are composed of CPW-based CRLH quarter-wave type resonators with two, three, and four unit cells originating from Figure 3, respectively. A 50 Ω CPW transmission line along with a stub and a coupled gap is used as the feed network. Both the stub and the coupled gap play important roles in impedance matching. With short-end of the CRLH TL, a loop configuration is formed by the top patches with gaps, the edged ground plane, and the shorted stub. According to the analysis in Section 2, dual-band, tri-band, and quad-band operations with negative resonance modes will be achieved for these loop antennas, respectively.

Full-wave electromagnetic simulations are carried out using Ansoft HFSS, and the reflection coefficients of the three antennas are given in Figure 5. For the dual-band loop antenna, the $n = -1, -3$ resonance modes corresponding to $f_{-1} = 2.39$ GHz and $f_{-3} = 1.94$ GHz are observed. The tri-band one gives three negative resonance modes $n = -1, -3, 5$ at $f_{-1} = 2.64$ GHz, $f_{-3} = 2.17$ GHz, and $f_{-5} =$

Table 1. Characteristics of the three multi-band loop antennas.

Mode		$n = -1$	$n = -3$	$n = -5$	$n = -7$
Dual-band	Frequency (GHz)	2.39	1.94	-	-
	Bandwidth (%)	6.0	1.7	-	-
	Size ($L \times W \times h$, λ_0)	$0.17 \times 0.14 \times 0.006$ @ $n = -3$			
	Frequency ratios	1.23			
Tri-band	Frequency (GHz)	2.64	2.17	1.92	-
	Bandwidth (%)	2.83	3.04	1.56	-
	Size ($L \times W \times h$, λ_0)	$0.18 \times 0.14 \times 0.006$ @ $n = -5$			
	Frequency ratios	1.22/1.13			
Quad-band	Frequency (GHz)	2.76	2.35	2.04	1.87
	Bandwidth (%)	1.74	1.79	1.77	1.07
	Size ($L \times W \times h$, λ_0)	$0.20 \times 0.13 \times 0.006$ @ $n = -7$			
	Frequency ratios	1.17/1.15/1.09			

1.92 GHz, respectively. The resonance frequencies of $n = -1, -3, -5, -7$ for the quad-band one occur at $f_{-1} = 2.76$ GHz, $f_{-3} = 2.35$ GHz, $f_{-5} = 2.04$ GHz, and $f_{-7} = 1.87$ GHz, respectively. The resonance frequencies corresponding to these modes can also be predicted from the dispersion diagram in Figure 3(b) at the frequencies where βd is equal to $n\pi/2N$. The slight deviation between the antenna's resonant frequencies and the resonant frequencies predicted from the dispersion diagram can be attributed to the addition of the shorted stub. Table 1 summarizes characteristics at each mode of the three multi-band loop antennas, such as resonance frequencies, antenna sizes, bandwidths ($VSWR \leq 2$), and frequency ratios (f_n/f_{n-2}). From this table, it can be seen that both size reduction and frequency ratios lower than 1.09 are achieved for the proposed antennas. Compared with conventional multi-band operations, the proposed approach provides an easier way

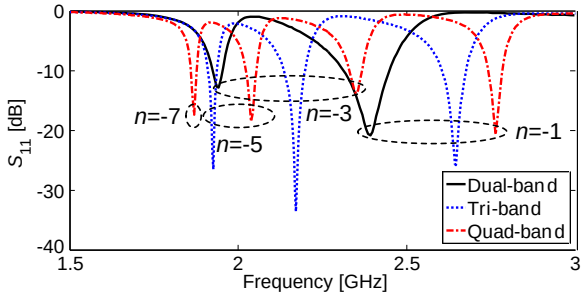

Figure 5. Simulated reflection coefficients of the proposed antennas.

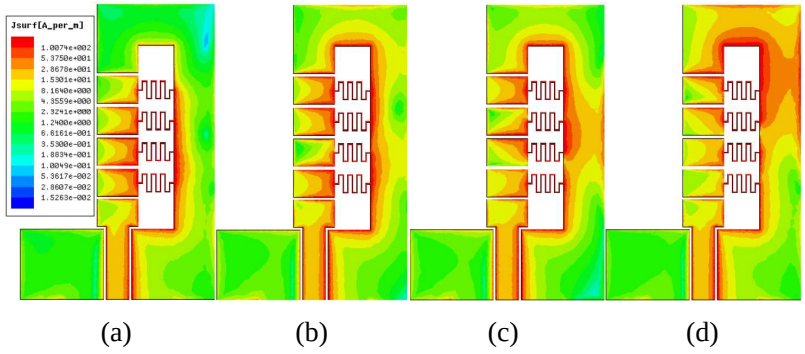

Figure 6. Simulated surface current distributions of the quad-band antenna at (a) 1.87, (b) 2.04, (c) 2.35, and (d) 2.76 GHz.

to realize multi-band antennas with low frequency ratios while keeps a compact size. In addition, more resonance frequencies with low frequency ratios can be arbitrarily obtained by modifying the proposed unit cell and/or its number without seriously sacrificing the entire size.

For giving a good physical insight into the behavior of the proposed antennas, the simulated surface current distributions of the quad-band one at 1.87, 2.04, 2.35, and 2.76 GHz are shown in Figure 6. As expected at these frequencies, the strong resonant currents flow mainly along with the meander lines, the edge of gaps, and the edge of center rectangle slot. This also means that the proposed antennas' performances are strongly influenced by the values of left-handed parameters (L_L, C_L). Obviously, for the lowest band excitation (1.87 GHz), most of the surface current is located along the lower half of the structure, whereas for the highest band excitation (2.76 GHz), the current distribution becomes more concentrated along the upper half of the structure. It is important to note that currents through adjacent turns of the meander lines are canceled at far field due to their opposite directions. This cancelation is possible because the separation between adjacent turns is very small ($g_1 < \lambda_0/4$).

4. FABRICATION AND MEASUREMENT

To validate the proposed approach, the tri-band prototype was fabricated on a FR-4 substrate ($\varepsilon_r = 4.4$, $\tan\delta = 0.02$) without a via process, as shown in Figure 7(a). The antenna can be easily matched to the 50 Ω CPW feedline without the employment of an external matching network or balun. It is important to note that the small CPW ground plane also contributes to the radiation of the antenna, since

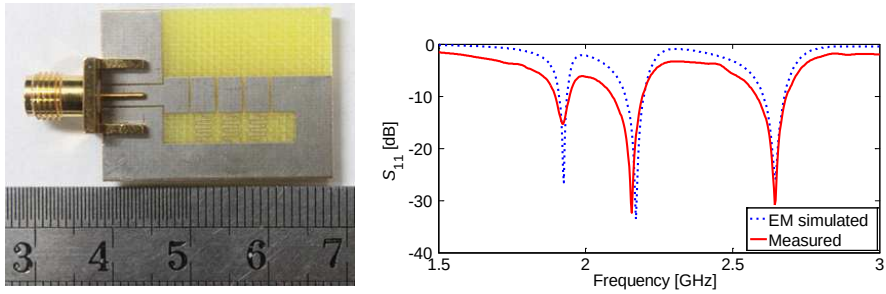

(a) (b)

Figure 7. (a) Photograph of the fabricated tri-band loop antenna. (b) Measured reflection coefficient of the fabricated tri-band loop antenna.

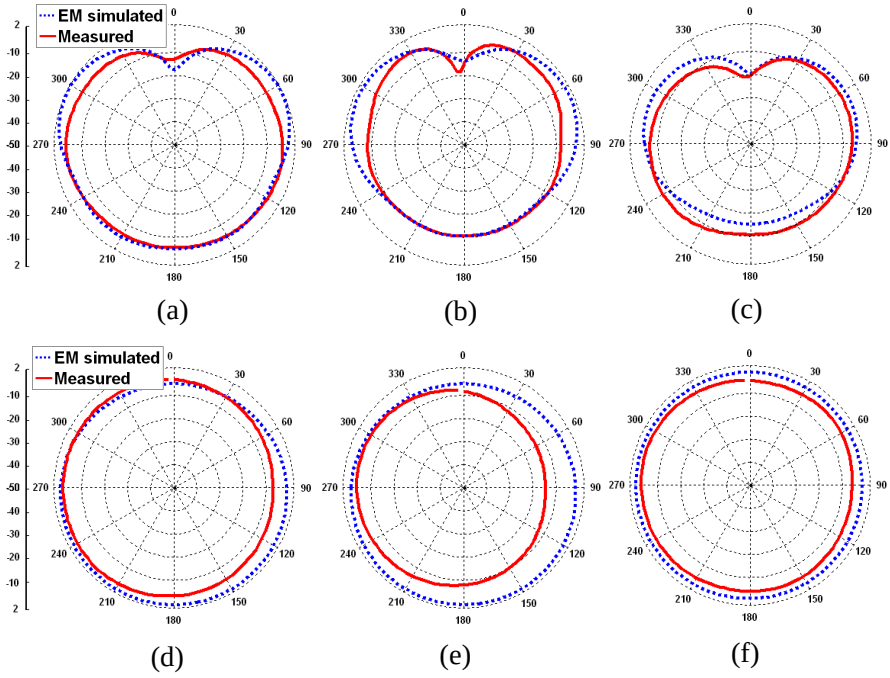

Figure 8. Simulated and measured radiation patterns of the tri-band loop antenna. (a) E-plane at $n = -1$ mode. (b) E-plane at $n = -3$ mode. (c) E-plane at $n = -5$ mode. (d) H-plane at $n = -1$ mode. (e) H-plane at $n = -3$ mode. (f) H-plane at $n = -5$ mode.

there are unbalanced currents due to its asymmetrical structure. The measured reflection coefficient obtained from Agilent network analyzer E5071C is given in Figure 7(b). The resonance frequencies of -1, -3, and -5 mode are measured to be 2.64 GHz, 2.15 GHz, and 1.92 GHz with all return losses above 15 dB, respectively, which coincide with the simulated. It can be seen that the antenna exhibits a wider bandwidth at each mode compared with the simulated. This may be attributed to the degradation of quality factor ($BW \propto 1/Q$), due to great dielectric loss of the substrate ($\tan\delta = 0.02$) and metal loss introduced by the narrow meander lines ($w_1 = 0.1$ mm).

Figure 8 shows the simulated and measured radiation patterns on the E-plane (x-z) and H-plane (y-z) at each mode. The antenna demonstrates similar omni-directional radiation patterns within the three operating bands due to the similar effective apertures and current distributions. Since the shorted stub is relative small, the currents along the two vertical edges of center rectangle slot make most

Table 2. Experimental results of the tri-band loop antenna.

Mode	Frequency (GHz)	Bandwidth (MHz)	Gain (dBi)	Efficiency
$n = -1$	2.64	105 (3.98%)	−1.48	43%
$n = -3$	2.15	105 (4.88%)	−1.29	38%
$n = -5$	1.92	51 (2.66%)	−1.69	33%

contribution to the radiation, thus the loop antenna operates as two closely spaced monopoles. Using the two principal pattern cuts, the measured gains using comparison method are negative, and resulting in a measured efficiency not exceeding 50%. This may be caused by the electrically small aperture size as well as the dielectric loss and metal loss. Another reason may be that currents on meander lines flowing in the opposed direction are eliminated at far field. Efficiency can be improved by using low-loss substrate and wider meander lines as well as new types of inductors, such as planar spiral inductors. The experimental results of the tri-band loop antenna are also listed in Table 2.

5. CONCLUSION

In this paper, a CPW-based CRLH quarter-wave type resonator has been proposed. The resonant characteristics of the resonator are analyzed by dispersion diagram of the CRLH TL unit cell. By taking advantage of its compact and dispersion-controllable features, three multi-band loop antennas are designed on a vialess single layer. Both size reduction and low frequency ratios have been achieved for the three prototypes. By modifying the unit cell and/or its number, more working frequencies with low frequency ratios can be arbitrarily chosen without seriously sacrificing the entire size. The tri-band prototype with a compact size of $0.18\lambda_0 \times 0.14\lambda_0 \times 0.006\lambda_0$ is fabricated and measured, exhibiting good impedance matching as well as stably omni-directional radiation patterns at each mode. The results show that the proposed approach would be helpful to design compact multi-band antennas with low frequency ratios for specific applications.

ACKNOWLEDGMENT

This work is supported by the National Natural Science Foundation of China (No. 60990320; 60990323) and the National 863 Project of China (No. 2012AA012305).

REFERENCES

1. Wong, K. L., *Planar Antennas for Wireless Communications,* John Wiley & Sons, Inc., 2003.
2. Kim, Y. and D. H. Kwon, "CPW-fed planar ultra wideband antenna having a frequency band notch function," *Electronics Letters*, Vol. 40, 403–405, 2004.
3. Song, K., Y. Z. Yin, and B. Chen, "Triple-band open L-slot antenna with a slit and a strip for WLAN/WiMAX applications," *Progress In Electromagnetics Research Letters*, Vol. 22, 139–146, 2011.
4. Hu, W., Y. Z. Yin, P. Fei, and X. Yang, "Compact triband square-slot antenna with symmetrical L-strips for WLAN/WiMAX applications," *IEEE Antennas and Wireless Propagation Letters*, Vol. 10, 462–465, 2011.
5. Jaw, J.-L. and J.-K. Chen, "CPW-fed hook-shaped strip antenna for dual wideband operation," *Journal of Electromagnetic Waves and Applications*, Vol. 22, No. 13, 1809–1818, 2008.
6. Heidari, A. A., M. Heyrani, and M. Nakhkash, "A dual-band circularly polarized stub loaded microstrip patch antenna for GPS applications," *Progress In Electromagnetics Research*, Vol. 92, 195–208, 2009.
7. Wang, E., J. Zheng, and Y. Liu, "A novel dual-band patch antenna for WLAN communication," *Progress In Electromagnetics Research C*, Vol. 6, 93–102, 2009.
8. Ciais, P., R. Staraj, G. Kossiavas, and C. Luxey, "Design of an internal quad-band antenna for mobile phones," *IEEE Microwave and Wireless Components Letters*, Vol. 14, 148–150, 2004.
9. Risco, S., J. Anguera, A. Andúar, A. Pérez, and C. Puente, "Coupled monopole antenna design for multiband handset devices," *Microwave and Optical Technology Letters*, Vol. 52, 359–364, 2010.
10. Zhang, S. M., F. S. Zhang, W. M. Li, W. Z. Li, and H. Y. Wu, "A multi-band monopole antenna with two different slots for WLAN and WiMAX applications," *Progress In Electromagnetics Research Letters,* Vol. 28, 173–181, 2012.
11. Song, Y., Y. C. Jiao, G. Zhao, and F. S. Zhang, "Multiband CPW-fed triangle-shaped monopole antenna for wireless applications," *Progress In Electromagnetics Research,* Vol. 70, 329–336, 2007.
12. Hossa, R., A. Byndas, and M. E. Bialkowski, "Improvement of compact terminal antenna performance by incorporating open-end slots in ground plane," *IEEE Microwave and Wireless*

Components Letters, Vol. 14, 283–285, 2004.

13. Abedin, M. F. and M. Ali, "Modifying the ground plane and its effect on planar inverted-F antennas (PIFAs) for mobile phone handsets," *IEEE Antennas and Wireless Propagation Letters*, Vol. 2, 226–229, 2003.
14. Anguera, J., I. Sanz, J. Mumbrú, and C. Puente, "Multi-band handset antenna with a parallel excitation of PIFA and slot radiators," *IEEE Transactions on Antennas and Propagation*, Vol. 58, 348–356, 2010.
15. Abdallah, M., F. Colombel, G. Le Ray, and M. Himdi, "Frequency tunable antenna for digital video broadcasting handheld application," *Progress In Electromagnetics Research Letters*, Vol. 24, 1–8, 2011.
16. Huang, L. and P. Russer, "Electrically tunable antenna design procedure for mobile applications," *IEEE Transactions on Microwave Theory and Techniques*, Vol. 56, 2789–2797, 2008.
17. A. Andújar, J. Anguera, and C. Puente, "Ground plane boosters as a compact antenna technology for wireless handheld devices," *IEEE Transactions on Antennas and Propagation*, Vol. 59, 1668–1677, 2011.
18. Veselago, V. G., "The electrodynamics of substances with simultaneously negative values of ε and μ," *Soviet Physics Uspekhi*, Vol. 10, 509–514, 1968.
19. Eleftheriades, G. V. and K. G. Balmain, *Negative-refraction Metamaterials: Fundamental Principles and Applications,* John Wiley & Sons, Inc., 2005.
20. Caloz, C. and T. Itoh, *Electromagnetic Metamaterials: Transmission Line Theory and Microwave Applications,* John Wiley & Sons, Inc., 2006.
21. Ntaikos, D. K., N. K. Bourgis, and T. V. Yioultsis, "Metamaterial-based electrically small multiband planar monopole antennas," *IEEE Antennas and Wireless Propagation Letters*, Vol. 10, 963–966, 2011.
22. Montero-de-Paz, J., E. Ugarte-Muñoz, and F. J. Herraiz-Martínez, "Multifrequency self-diplexed single patch antennas loaded with split ring resonators," *Progress In Electromagnetics Research*, Vol. 113, 47–66, 2011.
23. Du, G., X. Tang, and F. Xiao, "Tri-band metamaterial-inspired monopole antenna with modified S-shaped resonator," *Progress In Electromagnetics Research Letters*, Vol. 23, 39–48, 2011.

24. Caloz, C., T. Itoh, and A. Rennings, "CRLH metamaterial leaky-wave and resonant antennas," *IEEE Antennas and Propagation Magazine*, Vol. 50, 25–39, 2008.
25. Anghel, A. and R. Cacoveanu, "Improved composite right/left-handed cell for leaky-wave antenna," *Progress In Electromagnetics Research Letters*, Vol. 22, 59–69, 2011.
26. Jang, T., J. Choi, and S. Lim, "Compact coplanar waveguide (CPW)-fed zeroth-order resonant antennas with extended bandwidth and high efficiency on vialess single layer," *IEEE Transactions on Antennas and Propagation*, Vol. 59, 363–372, 2011.
27. Xiao, S., D. Wang, C. Wei, and B. Wang, "A compact planar negative permittivity ZOR antenna," *Journal of Electromagnetic Waves and Applications*, Vol. 25, Nos. 8–9, 1122–1130, 2011.
28. Ryu, Y. H., J. H. Park, J. H. Lee, and H. S. Tae, "Multi-band antenna using +1, −1, and 0 resonant mode of DGS dual composite right/left-handed transmission line," *Microwave and Optical Technology Letters*, Vol. 51, 2485–2488, 2009.
29. Yang, T., P. L. Chi, and T. Itoh, "Compact quarter-wave resonator and its applications to miniaturized diplexer and triplexer," *IEEE Transactions on Microwave Theory and Techniques*, Vol. 59, 260–269, 2011.
30. Bahl, I., *Lumped Elements for RF and Microwave Circuits,* Artech House Publishers, 2003.
31. Kim, D. and J. Yeo, "A passive RFID tag antenna installed in a recessed cavity in a metallic platform," *IEEE Transactions on Antennas and Propagation*, Vol. 58, 3814–3820, 2010.